Received: 14 November 2018 | Revised: 19 February 2019 | Accepted: 15 March 2019

DOI: 10.1002/term.2857

RESEARCH ARTICLE

WILEY

# Human gingival mesenchymal stem cells pretreated with vesicular moringin nanostructures as a new therapeutic approach in a mouse model of spinal cord injury

Santa Mammana[1] | Agnese Gugliandolo[1] | Eugenio Cavalli[1] | Francesca Diomede[2] | Renato Iori[3] | Romina Zappacosta[4] | Placido Bramanti[1] | Pio Conti[5] | Antonella Fontana[4] | Jacopo Pizzicannella[6] | Emanuela Mazzon[1]

[1] Department of Experimental Neurology, IRCCS Centro Neurolesi Bonino-Pulejo, Messina, Italy

[2] Stem Cells and Regenerative Medicine Laboratory, Department of Medical, Oral, and Biotechnological Sciences, University "G. d'Annunzio", Chieti, Italy

[3] Consiglio per la Ricerca in Agricoltura e l'Analisi dell'Economia Agraria, Centro di Ricerca Agricoltura e Ambiente (CREA-AA), Bologna, Italy

[4] Department of Pharmacy, University "G. d'Annunzio", Chieti, Italy

[5] Immunology Division, Postgraduate Medical School, University "G. d'Annunzio", Chieti, Italy

[6] Department of Medical, Oral and Biotechnological Sciences, University "G. d'Annunzio", Chieti, Italy

**Correspondence**
Emanuela Mazzon, Department of Experimental Neurology, IRCCS Centro Neurolesi Bonino-Pulejo, Contrada Casazza, 98123 Messina, Italy.
Email: emazzon.irccs@gmail.com

## Abstract

Spinal cord injury (SCI) is a neurological disorder that arises from a primary acute mechanical lesion, followed by a pathophysiological cascade of events that leads to further spinal cord tissue damage. Several preclinical and clinical studies have highlighted the ability of stem cell therapy to improve long-term functional recovery in SCI. Previously, we demonstrated that moringin (MOR) treatment accelerates the differentiation process in mesenchymal stem cells inducing an early up-regulation of neural development associated genes. In the present study, we investigated the anti-inflammatory, anti-apoptotic, and regenerative effects of gingival mesenchymal stem cells (GMSCs) pretreated with nanostructured liposomes enriched with MOR in an animal model of SCI. SCI was produced by extradural compression of the spinal cord at levels T6–T7 in ICR (CD-1) mice. Animals were randomly assigned to the following groups: Sham, SCI, SCI + GMSCs ($1 \times 10^6$ cell/i.v.), SCI + MOR-GMSCs ($1 \times 10^6$ cell/i.v.). Our data show that MOR-treated GMSCs exert anti-inflammatory and anti-apoptotic activities. In particular, MOR-treated GMSCs are able to reduce the spinal cord levels of COX-2, GFAP, and inflammatory cytokines IL-1β and IL-6 and to restore spinal cord normal morphology. Also, MOR-treated GMSCs influenced the apoptotic pathway, by reducing Bax, caspase 3, and caspase 9 expressions.

**KEYWORDS**

anti-inflammatory effect, gingiva stem cell, liposomes, moringin, spinal cord injury, stem cells

## 1 | INTRODUCTION

Spinal cord injury (SCI) is a complex neurological disorder that arises after a primary acute mechanical lesion. After the mechanical injury, a cascade of events caused the expansion of the neuronal lesion and increases the deficits and the neurological symptoms. Inflammatory cells such as macrophages, microglia, T lymphocytes, and neutrophils infiltrate the lesion site disrupting the spinal blood barrier (Ahuja et al., 2017). Between 6 and 12 hr after the damage, these cells

Jacopo Pizzicannella and Emanuela Mazzon are co-senior authors.

activate the release of inflammatory cytokines, for example, tumor necrosis factor-α, interleukin (IL)-1α, IL-1β, and IL-6 (Ahuja et al., 2017; Nakamura, Houghtling, MacArthur, Bayer, & Bregman, 2003).

Administration of high doses of glucocorticoid, such as methylprednisolone sodium succinate, is considered the standard of care. Indeed, systemic steroid therapy increases the release of anti-inflammatory mediators and promotes neural cell survival (Bracken et al., 1997; Singh, Agarwal, Barrese, & Heary, 2012). However, although pharmacological, surgical, and rehabilitative interventions are used to treat patients, there is still the necessity to develop new pharmacologic therapies for the treatment of SCI.

Adult mesenchymal stem cells (MSCs), thanks to their properties, have shown a wide range of neuroprotective effects in various preclinical and clinical investigations in neurodegenerative diseases (Volkman & Offen, 2017; Wang, Qu, & Zhao, 2011) and also exhibit anti-inflammatory and immunomodulatory roles in several experimental autoimmune and inflammatory diseases (Zhao, Ren, & Han, 2016). MSCs are a group of cells with non-hemopoietic, self-renewal, and multipotent differentiation properties (Via, Frizziero, & Oliva, 2012). They can differentiate into osteoblasts, chondrocytes, adipocytes, cardiomyocytes, endothelial, and neuronal cells (Phinney & Prockop, 2007; Pizzicannella et al., 2018).

MSCs have emerged as the most promising stem cell type, due to a favorable and better ethical profile (Mahla, 2016), and they represent candidates for the treatment of SCI, based on their ability to provide trophic support, reduce the inflammatory responses and cell death, promote axon remyelination, form scaffolding, enhance plasticity, and improve locomotor recovery following mechanical trauma (Oliveri, Bello, & Biering-Sorensen, 2014). MSCs, administered via intravenous, intrathecal, intralesional, and intraspinal routes, have already shown to improve the animal conditions in SCI models (Shende & Subedi, 2017).

MSCs can be isolated from different tissues, including bone marrow, umbilical cord, placenta, adipose tissue, and human oral tissues (Hendijani, 2017). In the oral tissues, different human oral-derived stem cells have been described, such as dental pulp stem cells, exfoliated deciduous teeth stem cells, periodontal ligament stem cells, apical papilla stem cells, dental follicle stem cells, and gingival stem cells (GMSCs; Ballerini et al., 2017; Egusa, Sonoyama, Nishimura, Atsuta, & Akiyama, 2012; Giacoppo et al., 2017; Sharpe, 2016).

Mesenchymal stem cells derived from human gingiva (GMSC) are a good source of stem cells for the ease of accessibility and harvesting, homogeneity, higher proliferation rate, and stable characteristics (Sharpe, 2016). The gingival tissue has dense vasculature, high turnover rate, and regeneration capacity in vivo.

Furthermore, human gingival tissue origin from neural crest and contain neural crest-derived N-GMSCs that show the capacity to differentiate into neural cells and chondrocytes and to modulate immune cells (Diomede et al., 2017; Diomede et al., 2018; Xu et al., 2013).

*Moringa oleifera Lam*., belonging to the *Moringaceae* family, also known as "horseradish" tree, grows in many tropical and sub-tropical areas. These plants have been used in the traditional medicine for their beneficial properties, mainly due to the presence of glucosinolates, precursors of isothiocyanates. Moringin (4-(α-L-rhamnopyranosyloxy) benzylisothiocyanate) (MOR) results from the myrosinase hydrolysis of glucomoringin, the most abundant glucosinolate in *M. oleifera* seeds.

The phyto-compounds of *M. oleifera* showed a great ability to counteract neuroinflammation in murine models of experimental autoimmune encephalomyelitis and subacute Parkinson's disease (Giacoppo et al., 2016; Giacoppo et al., 2017).

In previous studies, we demonstrated that oral MSCs are able to differentiate spontaneously toward the neuronal cell lineage after the prolonged cellular expansion (Rajan et al., 2017), and the MOR treatment accelerates this differentiation process inducing an early up-regulation of neural development associated genes (Romeo et al., 2018).

Given the promising anti-inflammatory role of MOR and its capacity to promote neuronal differentiation, in the present study, we have investigated the anti-inflammatory, anti-apoptotic, and regenerative effects of GMSCs pretreated with nanostructured liposomes enriched with MOR in an animal model of SCI.

## 2 | MATERIALS AND METHODS

### 2.1 | Ethics statement

Ethical Committee of the Medical School, "G. d'Annunzio" University, Chieti, Italy, has approved the present research project (statement number 266/April 17, 2014). All subjects enrolled in the study signed the informed consent form before tissue collection. All the in vitro experiments were carried out at the Stem Cells and Regenerative Medicine Laboratory, "G. d'Annunzio" University, that are certified in accordance with the quality standard ISO 9001:2008 (32031/15/S).

### 2.2 | Isolation and culture of GMSCs

Gingival tissue biopsies were obtained from healthy adult volunteers with no gingival inflammation. The gingival specimens were completely de-epithelialized with a scalpel, for the exclusion of most of the keratinocytes resident in the gingiva. In brief, the connective tissues were then grounded and washed with phosphate buffered saline (PBS; EuroClone, Milan, Italy). Subsequently, cells were cultured using TheraPEAK™ MSCGM-CD™ BulletKit serum-free, chemically defined (MSCGM-CD) medium for the growth of human MSCs (Lonza, Basel, Switzerland). The medium was changed twice a week; cells are spontaneously migrating from the explant fragments and were trypsinized using Triple Select (LiStar Fish) after reaching about 80% of confluence (Libro et al., 2016).

### 2.3 | Moringin purification

Moringin was isolated from *M. oleifera* (fam. *Moringaceae*) seeds (cake powder PKM2 provided by Indena India Pvt. Ltd., Bangalore, India) at the Bologna laboratory (CREA-AA; previously CIN) using established methods, and the structure was confirmed by nuclear magnetic resonance spectroscopic analyses (Brunelli et al., 2010; Muller et al., 2015).

## 2.4 | Encapsulation of moringin in liposomes

Liposomes were prepared according to the following protocol (De Maria, Fontana, Gasbarri, & Velluto, 2006; Velluto, Gasbarri, Angelini, & Fontana, 2011; Viale et al., 2016; Zappacosta et al., 2010). An appropriate aliquot of 1-palmitoyl-2-oleoyl-glycerol-3-phosphocholine (POPC), dissolved in chloroform, was put in a round-bottomed flask and dried in a rotary evaporator under reduced pressure at 40°C to form a thin phospholipid film on the inside wall of the flask. The phospholipidic film was kept at 4°C overnight before rehydration with PBS buffer (pH 7.4) and sonication for 30 min. An appropriate amount of MOR in dimethyl sulfoxide was added to the resulting liposomal suspension in order to obtain a POPC to MOR ($5 \times 10^{-6}$ M) ratio of 25:1. In order to evaluate the MOR loading into the liposomes, we prepared a concentrated liposomal dispersion of MOR-enriched liposomes following the same protocol described above. The dispersion was filtrated through a Sephadex G-25 column in order to remove eventually unentrapped MOR. Liposomes were disrupted by the addition of $CHCl_3$, and MOR was quantified by UV–Vis spectrophotometry at wavelength 231 nm (extinction coefficient of MOR at 231 nm wavelength = 5529).

## 2.5 | Characterization of MOR-enriched liposomes

Liposomes were characterized in terms of dimensions and ζ-potential by using a Zeta Plus apparatus (Photon Correlation Spectroscopic and Zeta Potential Analyzer, Brookhaven Instruments Corporation). For stability measurements, the liposomes were analogously prepared, the only difference being the rehydration with a 50-mM solution of 5(6)-carboxyfluorescein (CF). Unentrapped CF was removed by filtration of the liposomal suspension through gel filtration by using a Sephadex G-25 column.

## 2.6 | Treatment of GMSCs with MOR

GMSCs were cultured in a monolayer using TheraPEAK_MSCGM-CD_BulletKit serum-free, chemically defined (MSCGM-CD) medium (Lonza, Basel, Switzerland) at 37°C in a moisturized atmosphere of 5% $CO_2$ and 95% air. For drug treatment, cells were grown until 70–80% confluence, and then, they were treated for 48 hr with a dispersion of MOR embedded in liposomes. In particular, the stock solution of MOR embedded in liposomes contained MOR at the concentration $5 \times 10^{-6}$ M. The solution was diluted 10 μl/ml of medium in order to obtain a final concentration of 0.05-μM MOR.

In order to evaluate liposome internalization in GMSCs and, consequently, the capability of MOR to be delivered into the cell, liposomes, with and without MOR, were loaded with the hydrophilic fluorescent green marker (CF) at a concentration of 0.025 mg/ml, by rehydrating the proper thin phospholipid film with a PBS solution of 0.025-mg/ml CF. Liposomes were then filtered through Sephadex G-25 in order to remove the unentrapped probe. GMSCs were treated with such liposomal dispersions for 24 hr, and the internalization of fluorescent vesicles was monitored by confocal microscopy CLSM800 (Zeiss, Jena, Germany) using 470/535 nm as fluorescence excitation/emission wavelengths (Diomede et al., 2018).

## 2.7 | Scanning electron microscopy analysis

The morphology of the GMSCs and GMSCs + MOR was examined using a scanning electron microscope (EVO50 XVP, Zeiss). Cells grown on coverslips were fixed for 4 hr at 4°C in 4% glutaraldehyde in 0.05-M phosphate buffer (pH 7.4), dehydrated in increasing ethanol concentrations, and then critical point dried (Pizzicannella, Cavalcanti, Trubiani, & Diomede, 2018). The samples were mounted on aluminum stubs and coated with a gold layer using a sputter coater (Emitech Ltd., Ashford, UK) and were visualized at scanning electron microscopy (SEM; Diomede et al., 2016).

## 2.8 | Cell metabolic activity and viability analysis

3-(4,5-Dimethylthiazol-2-yl)-5-(3-carboxymethoxyphenyl)-2-(4-sulfophenyl)-2*H*-tetrazolium (MTS) assay (CellTiter 96® AQueous One Solution Cell Proliferation Assay; Promega Corporation, Fitchburg, WI, USA) was used to measure the metabolic activity of the cells. Twenty microliters of MTS were added to 200 μl of fresh medium per well. The plates were incubated for 4 hr at 37°C and 5% $CO_2$. Then, the results were measured by spectrophotometry in 200 μl per well, using a multimode microplate reader (Synergy HT; BioTek, Winooski, VT, USA) at 490 nm, with a reference at 690 nm (Cavalcanti et al., 2015). Moreover, the doubling time of the Trypan blue harvested cells, at 24, 48, 72 hr, and 1 week of culture, was calculated by using an algorithm available online (www.doubling-time.com; Diomede et al., 2017).

## 2.9 | Analysis of cell culture medium for western blot of IL-10 and TGF-β

After 48 hr, the cell culture medium was collected and centrifugated in order to remove cell debris. For protein quantification, 1 ml of cell culture medium was added with 4 ml of cold acetone, incubated for 1 hr at −20°C, and centrifuged at 14,000 *g* for 12 min at 4°C. The resulted pellet was resuspended in radioimmunoprecipitation assay buffer and quantified for protein concentration using Bio-Rad Protein Assay (Bio-Rad, Segrate, Italy). Proteins were subjected to SDS-PAGE, followed by blotting with polyvinylidene fluoride (PVDF) membranes (Immobilon-P transfer membrane; Millipore). PVDF membranes were incubated in 5% skimmed milk in 1× PBS for 1 hr at room temperature. After, membranes were incubated with the following primary antibodies overnight at 4°C: TGF-β (1:250; Abcam) and IL-10 (1:100; Santa Cruz Biotechnology). Membranes were then incubated with horseradish peroxidase (HRP)-conjugated anti-mouse or anti-rat IgG secondary antibody (1:2,000; Santa Cruz Biotechnology) for 1 hr at room temperature. In order to verify the equal loading of proteins, membranes were stained with Ponceau S. Images of protein bands were visualized using an ECL system (Luminata Western HRP Substrates; Millipore),

acquired by ChemiDoc MP System (Bio-Rad) and quantified using a computer program (ImageJ; National Institutes of Health, Bethesda, MD, USA).

## 2.10 | Immunocytochemistry

After 48 hr of treatment with MOR, GMSCs, grown on coverslips (10 mm, Thermo Scientific, Germany), were fixed with 4% paraformaldehyde at room temperature for 20 min and then washed with PBS (pH 7.5). Then, GMSCs were incubated with 3% hydrogen peroxide ($H_2O_2$) at room temperature for 15 min in order to suppress the endogenous peroxidase activity. After washing with PBS, GMSCs were blocked with normal horse serum +0.1% Triton X-100 for 20 min followed by incubation overnight at 4°C with the following primary antibodies: TGF-β (1:200, Abcam), IL-10 (1:50, Santa Cruz Biotechnology Inc.), IL-1β (1:250, Cell Signaling Technology), COX-2 (1:50 Santa Cruz Biotechnology Inc.), p38 (1:250, Cell Signaling Technology), and MMP9 (1:200, Abcam). After PBS wash, cells were incubated with the biotinylated secondary antibody (1:200, Vector Laboratories, Burlingame, CA, USA) and streptavidin ABComplex-HRP (ABC-kit from Dako, Glostrup, Denmark). The immunostaining was developed with a peroxidase substrate kit DAB (Vector Laboratories; brown color; positive staining) and counterstaining with nuclear fast red (Vector Laboratories; pink background; negative staining). Microscopy was performed using light microscopy (LEICA DM 2000 combined with LEICA ICC50 HD camera; Pizzicannella, Rabozzi, Trubiani, & Di Giammarco, 2011). Immunocytochemistry images were assessed for densitometry analysis using LEICA Application Suite V4.2.0 software to calculate the percentage of positive staining of the cells. All images are representative of three independent experiments.

## 2.11 | Animals

ICR (CD-1) mice (male, 25–30 g) were purchased from Envigo (Pietro al Natisone, Udine, Italy). Animals have housed in individually ventilated cages with ad libitum food and water, and they are allowed to adapt for at least 1 week to their environment before commencing the study. The room was maintained at a constant temperature (21 ± 2°C) and humidity (50 ± 0%) on a 12 hr/12 hr light/dark cycle. Protection of animals used in the experiment is in accordance with Directive 2010/63/UE, enforced by the Italian D. Lgs 26/2014. Physical facilities and equipment for accommodation and care of animals are in accordance with the provisions of EEC Council Directive 86/609.

## 2.12 | Surgical procedures

The animals were anesthetized with an anesthetic cocktail composed of tiletamine plus xylazine (10 mg/kg, i.p.). Before surgery, their backs were shaved and disinfected with Betadine Surgical Scrub followed by 10% povidone–iodine solution.

A longitudinal incision was made on the midline of the back, exposing the paravertebral muscles. Laminectomy was performed using a pair of fine forceps at the T5–T8 levels to expose the dorsal side of the spinal column.

SCI was produced by extradural compression of the spinal cord at levels T6–T7 using an aneurysm clip with a closing force of 24 *g*. In all injured groups, the spinal cord was compressed for 1 min. The animals were kept on a heated mat (35°C) until fully recovered from anesthesia, and after that, they were housed in a temperature-controlled cage. The animals were sacrificed on Day 14 post-surgery, by intravenous administration of Tanax (5 ml/kg body weight), and the spinal cord tissues were harvested.

Five (two for the sham group) spinal cord for each group were fixed in 10% (w/v) in PBS-buffered formaldehyde for histological studies, and the remaining five (three for the sham group) were stored at −20°C for protein extraction.

## 2.13 | Treatment

A total of 35 mice were randomly divided into the following four groups:

1. Sham group ($n$ = 5) received the surgical procedure without SCI;
2. SCI group ($n$ = 10) mice received an endovenous injection, into the tail vein, (200 µl) of PBS 1 hr post-injury;
3. GMSC group (SCI + intravenous treatment; $n$ = 10) mice received an intravenous injection, into the tail vein, of the stem cells ($1 \times 10^6$ cells per mouse resuspended in 200 µl of PBS) 1 hr post-injury; and
4. GMSC + MOR group (SCI + intravenous treatment; $n$ = 10) received an intravenous injection, into the tail vein, of the stem cells pretreated with liposomes enriched with MOR ($1 \times 10^6$ cells per mouse resuspended in 200 µl of PBS) 1 hr post-injury.

## 2.14 | Clinical assessment

The Basso mouse scale (BMS) test was used to evaluate functional recovery after SCI as previously described (Basso et al., 2006) for SCI, SCI + GMSC, SCI + GMSC + MOR, and Sham conditions. Clinical signs were monitored daily starting from Day 1 post-injury. The scale ranges from 0 that indicates complete paralysis to 9 points that indicate normal hindlimb function. The animals were examined individually, and BMS scoring was performed by two blinded observers for 4 min per animal.

## 2.15 | Light microscopy

On the 14th day of SCI induction, spinal cord tissues were sampled and fixed in 10% (w/v) in PBS-buffered formaldehyde, embedded in paraffin, and then cut into sections 7 µm thick. The sections were deparaffinized with xylene, rehydrated, and stained with

hematoxylin–eosin to be studied by an optical microscope (Leica microscope ICC50HD).

### 2.16 | Immunohistochemistry of mouse spinal cord tissues

Paraffin-embedded spinal cord tissue sections were deparaffinized using xylene, rehydrated with alcohol series, and incubated in 0.01-M citrate buffer (pH 6) for 4 min to retrieve antigen. Afterward, sections were incubated with 0.3% (v/v) $H_2O_2$ in 60% (v/v) methanol for 30 min to quench endogenous peroxidase and blocked with normal goat serum in PBS (2% [v/v]) for 20 min. Next, sections were incubated with the following primary antibodies overnight at 4°C:

- anti-Bax (1:100; Santa Cruz Biotechnology);
- anti-Bcl-2 (1:100; Santa Cruz Biotechnology);
- anti-cleaved caspase 3 (1:250; Cell Signaling Technology);
- anti-caspase 9 (1:250; Cell Signaling Technology);
- anti-GFAP (1:100; Santa Cruz Biotechnology);
- anti-IL6 (1:250; Cell Signaling Technology); and
- anti-IL-1β (1:100; Santa Cruz Biotechnology).

After washing with PBS, sections were incubated with avidin/biotin blocking reagent (DBA, Segrate, Italy) to block endogenous avidin and biotin binding sites. Next, sections were incubated with universal biotinylated secondary antibody followed by avidin–HRP-conjugated solution (Vectastain ABC Kit; Vector Laboratories) according to the manufacturer's instructions. Sections were then incubated with a hydrogen peroxide/DAB kit (Vector Laboratories) according to the manufacturer's instructions. Counterstaining was performed with nuclear fast red (Vector Laboratories; pink background). To verify nonspecific background, immunostaining sections were incubated with either primary or secondary antibody alone, and no staining was evidenced. Immunohistochemical images were acquired using light microscopy (Leica DM 2000 combined with LEICA ICC50 HD camera) and assessed by densitometric analysis by Leica Application Suite V4.2.0 software.

### 2.17 | Western blot analysis of mouse spinal cord tissues

Spinal cord tissues were homogenized using ice-cold lysis buffer (10-mM Tris–HCl, pH-7.4, 0.32-M sucrose, 2-mM EDTA, 1-mM EGTA, 50-mM NaF, 5-mM NaN3, 10-mM 2-ME) with protease inhibitor tablets (Roche Applied Science, Monza, Italy). Homogenates were kept on ice for 15 min, and after, they were centrifugated at 1,000 *g* for 10 min at 4°C, and the resulting supernatant was collected as the cytoplasmic fraction. Pellets were further lysed with ice-cold extraction buffer (10-mM Tris–HCl, pH 7.4, 150-mM NaCl, 1-mM EDTA, 1-mM EGTA, 1% Triton X-100) and protease inhibitors. Homogenates were centrifugated at 15,000 *g* for 30 min at 4°C. The resulting supernatant was collected as nuclear fraction. Protein concentrations were evaluated using the Bio-Rad Protein Assay (Bio-Rad). Proteins were subjected to SDS-PAGE, followed by blotting with PVDF membranes (Immobilon-P transfer membrane; Millipore). PVDF membranes were incubated in 5% skimmed milk in 1× PBS for 1 hr at room temperature. After, membranes were incubated with the following primary antibodies overnight at 4°C: cyclooxygenase-2 (COX-2, 1:250; Santa Cruz Biotechnology) and IL-1β (1:500; Cell Signaling Technology). Membranes were then incubated with HRP-conjugated anti-mouse IgG secondary antibody (1:2,000; Santa Cruz Biotechnology) for 1 hr at room temperature. In order to verify the equal loading of proteins, membranes were stripped and reprobed with HRP-conjugated glyceraldehyde 3-phosphate dehydrogenase antibody (1:1,000; Cell Signaling Technology). Images of protein bands were visualized using an ECL system (Luminata Western HRP Substrates; Millipore), acquired by ChemiDoc MP System (Bio-Rad) and quantified using a computer program (ImageJ; National Institutes of Health).

### 2.18 | Statistical analysis

Statistical analysis of the data was carried out using GraphPad Prism version 7.0 program (GraphPad Software, La Jolla, CA). Statistical significance was measured by one-way or two-way analysis of variance and post hoc Bonferroni test for multiple comparisons or Student's *t*-test for the comparison between two groups. A $p$ value less than .05 was considered statistically significant. Results are expressed as mean ± standard error of the mean.

## 3 | RESULTS

### 3.1 | Characterization of moringin-enriched liposomes and their internalization in GMSCs

The spectrophotometric determination of MOR in disrupted liposomes evidenced the complete embedding of MOR in the liposomes (Figure 1a). The presence of MOR in the liposomes did not alter their features significantly (Table 1). In particular, results confirmed that the lipophilic MOR solubilizes in the membrane bilayer of the liposomes. As a matter of fact, the surface charge, expressed as ζ-potential, kept its original negative value passing from −20.2 ± 0.9 mV in the pure POPC liposome to −19.8 ± 1.3 mV in the MOR-enriched ones, whereas the dimensions of the liposomes slightly increased passing from 248.5 ± 11.6 nm of the pure POPC liposomes to 325.0 ± 4.9 nm of the MOR-enriched liposomes. This enlargement was indicative of the fact that MOR located in the bilayer rather than in the aqueous core. The polydispersity did not change on MOR embedding. Eventually, even the stability of the liposomes, measured in terms of release of the CF dye embedded in the aqueous core, did not vary. The release constant was 4.45 (±0.27) × $10^{-5}$ $s^{-1}$ for pure POPC liposomes and 4.10 (±0.21) × $10^{-5}$ $s^{-1}$ for MOR-enriched ones.

The intracellular delivery of CF was monitored by measuring the intracellular green fluorescence increase. CF internalization could be monitored both (a) as “punctate” fluorescence in the perinuclear

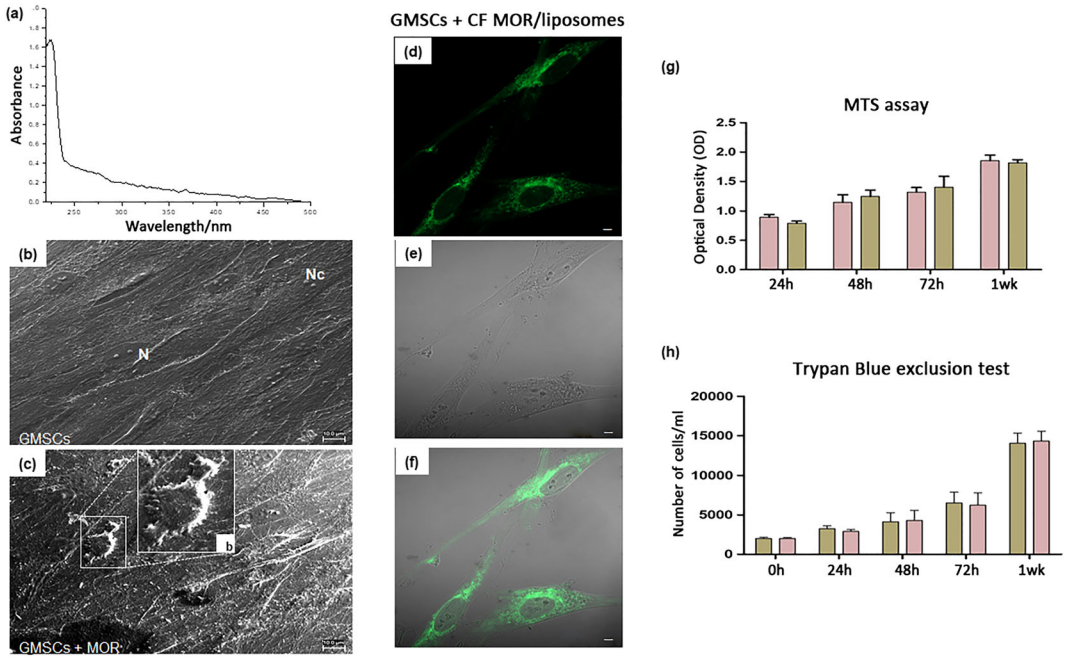


**FIGURE 1** Evaluation of internalization of liposomes in GMSCs and cell morphological aspects and metabolic activity. (a) UV–Vis spectrum of MOR in disrupted liposomes. (b) GMSCs and (c) GMSCs + MOR observed under SEM microscopy showed evident different morphological features; scale bar: 10 μm. (b) Cell with roundish shape and short elongation can be visible at high magnification. (d) Green fluorescent channel of GMSCs incubated for 24 hr with liposomes containing MOR stained with CF. (e) GMSCs observed at transmission light channel. (f) Merge image of two above mentioned channels. Magnification: 63×. Scale bar: 10 μm. (g) GMSCs and GMSCs + MOR metabolic activity evaluated using MTS assay. (h) GMSCs and GMSCs + MOR viability was evaluated using Trypan blue exclusion test. Values are expressed as mean ± standard error of the mean. N, nuclei; Nc, nucleoli [Colour figure can be viewed at wileyonlinelibrary.com]

**TABLE 1** Characterization of liposomes

| Samples | ζ-potential | Dimension | Polidispersity | Stability ($k/s^{-1}$) |
|---|---|---|---|---|
| POPC liposomes | −20.2 ± 0.9 | 248.5 ± 11.70 | 0.27 ± 0.01 | 4.45 (±0.27) × $10^{-5}$ |
| Moringin-enriched liposomes | −19.8 ± 1.3 | 325.0 ± 4.9 | 0.28 ± 0.01 | 4.10 (±0.21) × $10^{-5}$ |

compartment, likely related to a process of intact vesicle internalization and (b) as a cell-wide "diffuse" cytoplasmic fluorescence, due to the release of the vesicle content to the cytosol (Manconi, Isola, Falchi, Sinico, & Fadda, 2007; Figure 1d–f). The large number of fluorescent vesicles observed in the perinuclear area of GMSCc after 24 hr of incubation is indicative of internalization of intact liposomes that release CF in the cytosol only after their internalization. A slight signal could also be observed in the nuclei.

## 3.2 | GMSCs morphology, metabolic activity, and viability assay

GMSCs and GMSCs + MOR were observed under SEM. GMSCs showed a spindle-shaped morphology with long cytoplasmic process and filopodia taking contact with neighboring cells. At the cytoplasmic level, many cytoskeleton filaments and nuclei, containing one or more nucleoli, were evident (Figure 1b). On the other hand, the GMSCs + MOR acquired a roundish or elliptical shape detaching from the bottom of the coverslip. Cells appeared thinner when compared with the control cells, and several short cytoplasmic processes were present (Figure 1c). A cell with roundish shape and short elongation can be visible at high magnification (Figure 1b, inset).

The metabolic activity and cell number were monitored for a week to test the influence of MOR treatment on GMSCs. The metabolic activity of the GMSCs and GMSCs + MOR was determined by means of an MTS assay. No difference in terms of optical density recorded data was observed at 24, 48, 72 hr and 1 week of culture. However, the cell metabolic activity increased throughout the experimental period on GMSCs and GMSCs + MOR (Figure 1g). The metabolic activity data were confirmed by means Trypan blue exclusion test staining that showed a logarithmic growth during the period of culture, but no statistically significant differences were revealed among the two considered group (Figure 1h). Each experiment was repeated in triplicate.

## 3.3 | GMSCs pretreated with MOR promoted recovery of motor function and restored spinal cord morphology in SCI model

In order to evaluate the efficacy of GMSCs and GMSCs + MOR in the treatment of SCI, after the induction of spinal cord damage, cells were

injected into the tail vein. Mice were scored daily and were sacrificed after 2 weeks.

Hindlimb motor function was not improved in SCI groups at various time points. However, BMS score was significantly increased in GMSCs and GMSCs + MOR-treated groups compared with SCI. However, the administration of GMSCs + MOR in SCI animals induced a precocious and better recovery of locomotor function. Indeed, these animals showed a significant increase in score since Day 4 after injury. Instead, in SCI mice injected with GMSCs alone, a significant improvement became evident at Day 8 post-injury.

Also, BMS scores of mice treated with GMSCs + MOR were higher compared with those of GMSC-treated groups, reaching a statistically significant difference since Day 9 post-injury. Therefore, MOR enhanced recovery of hindlimb motor function (Figure 2a).

Hematoxylin–eosin evidenced the loss of the normal spinal cord morphology in mice subjected to SCI (Figure 2b). GMSCs administration partially improved the morphology of the spinal cord in SCI animals. Interestingly, the injection of GMSCs + MOR restored the normal spinal cord morphology (Figure 2b).

### 3.4 | GMSCs pretreated with MOR were able to counteract inflammation and apoptosis in SCI models

The spinal cord of SCI mice showed a significantly higher expression of the COX-2 protein, as evaluated by western blot (Figure 2c). The injection of both GMSCs alone or pretreated with MOR in SCI mice was able to reduce COX-2 protein to levels similar to that of sham animals (Figure 2c).

Moreover, we observed positive staining for IL-6 and IL-1β in spinal cord tissues of SCI mice through immunohistochemistry (Figure 3). The injection of GMSCs partially reduced the expression of the two pro-inflammatory ILs in SCI mice, whereas no positivity in the spinal cord of SCI mice administered with GMSCs + MOR and in sham mice was detected (Figure 3).

In accordance with the presence of inflammation in SCI animals, we observed a marked positivity of spinal cord tissues for GFAP (Figure 3). Spinal cords of mice with SCI injected with GMSCs showed a reduced expression of GFAP, and even a lower positivity was evidenced for mice administered with GMSCs + MOR (Figure 3). In particular, in this last group of mice, the positivity for GFAP was similar to that of sham animals (Figure 3).

These results indicated that GMSCs have a role in the reduction of inflammation, and pretreatment with MOR enhances the anti-inflammatory action.

In addition to inflammation, we observed an induction of the apoptotic pathway in SCI animals. In particular, SCI mice showed a marked positivity for the pro-apoptotic proteins BAX, cleaved caspase 3, and caspase 9 compared with sham animals in spinal cord tissues (Figures 4 and 5). However, GMSCs injection in SCI mice was able to partially diminish the expression of these apoptotic proteins. Furthermore, the group of animals with SCI injected with GMSCs + MOR

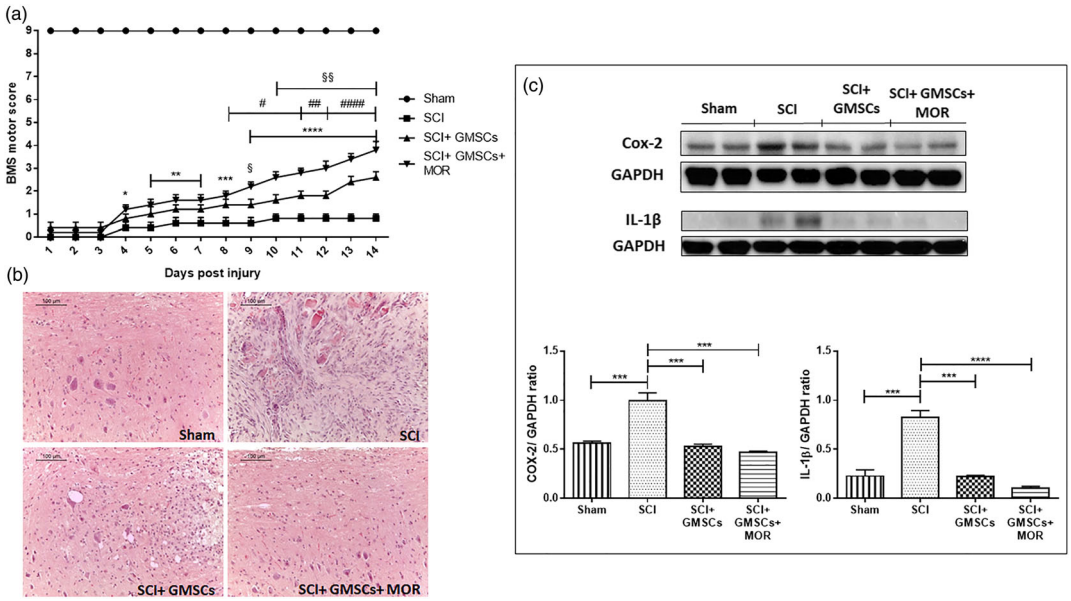


**FIGURE 2** Motor score, hematoxylin–eosin staining and western blot analysis for COX-2 and IL-1β with densitometric analysis in spinal cord tissues. (a) BMS motor score evidenced a modest recovery of motor function in SCI animal treated with GMSCs. A better and precocious recovery was evidenced in SCI mice injected with GMSCs + MOR. Sham mice showed a statistically significant difference compared with all other groups at all-time points ($p < .0001$). $^{*}p < .05$, $^{**}p < .01$, $^{***}p < .001$, $^{****}p < .0001$, SCI versus SCI + GMSCs + MOR; $^{\#}p < .05$, $^{\#\#}p < .01$, $^{\#\#\#\#}p < .0001$, SCI versus SCI + GMSCs; $^{\S}p < .05$, $^{\S\S}p < .01$, SCI + GMSCs versus SCI + GMSCs + MOR. (b) Hematoxylin–eosin staining showed that recovery of spinal cord normal morphology in SCI animals administered with GMSCs + MOR; scale bar: 100 μm; objective 10×. (c) The results evidenced an increased level of COX-2 and IL-1β in the spinal cord of SCI mice compared with sham animals. The injection of either GMSCs and GMSCs + MOR reduced the levels of COX-2 to levels similar to sham mice. IL-1β levels decreased in the spinal cord of SCI mice administered with GMSCs alone, but the injection of GMSCs + MOR induced a marked reduction. $^{***}p < .001$, $^{****}p < .0001$ [Colour figure can be viewed at wileyonlinelibrary.com]

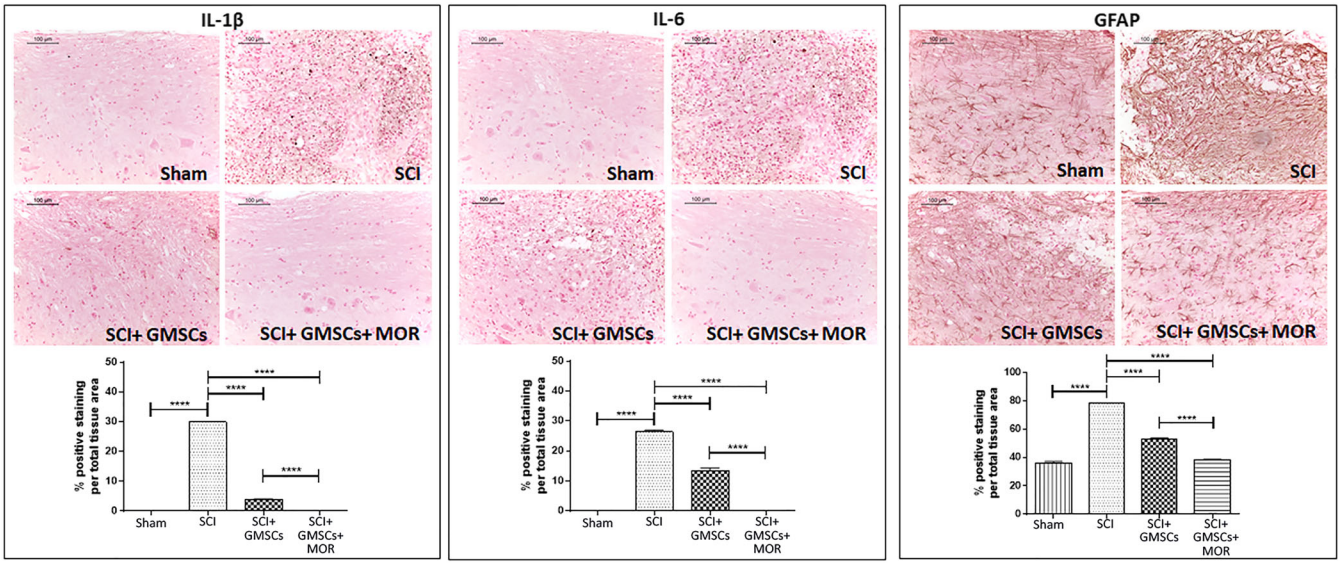


**FIGURE 3** Immunohistochemistry for IL-1β, IL-6, and GFAP with densitometric analysis. Immunohistochemistry evidenced the positive staining for IL-1β and IL-6 in the spinal cord of SCI mice compared with sham animals that showed negative staining. The administration of GMSCs and, in particular, of GMSCs + MOR reduced the expression of IL-1β and IL-6 in the spinal cord of SCI mice. A marked positivity for GFAP in the spinal cord of SCI mice was observed compared with sham animals. The administration of GMSCs in SCI mice reduced the expression of GFAP, whereas animals with SCI injected with GMSCs + MOR showed staining similar to sham animals. Scale bar: 100 μm; objective 10×. $^{****}p < .0001$ [Colour figure can be viewed at wileyonlinelibrary.com]

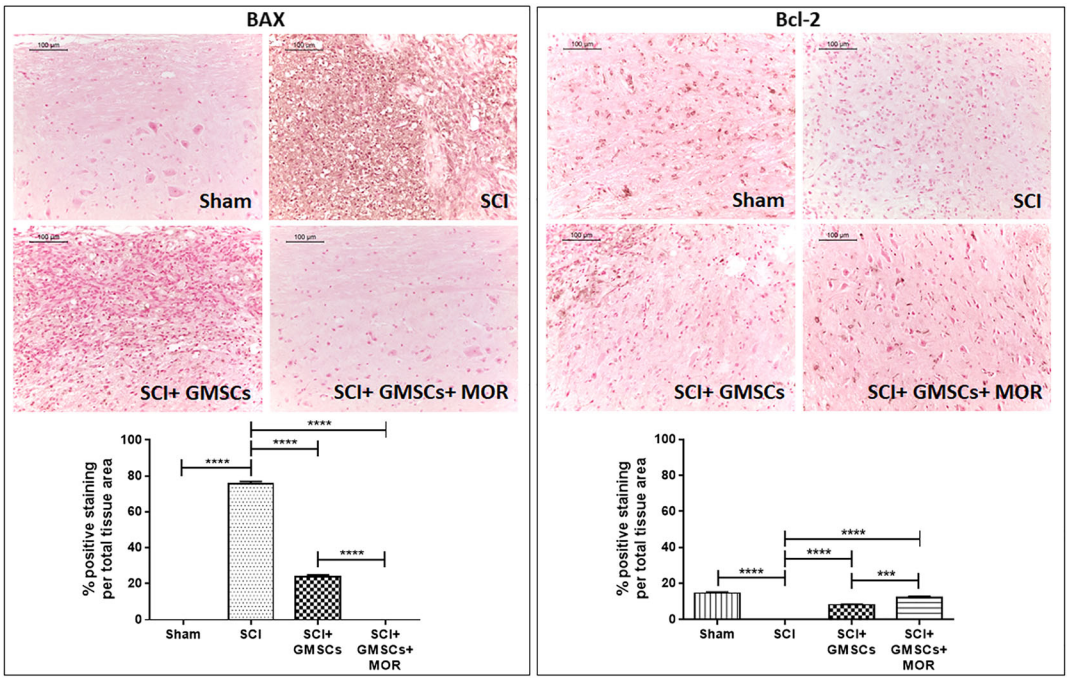


**FIGURE 4** Immunohistochemistry for Bax and Bcl-2 with densitometric analysis. Immunohistochemistry evidenced the positive staining for Bax and the negative expression for Bcl-2 in the spinal cord of SCI mice compared with sham animals. Instead, SCI mice injected with GMSCs or GMSCs + MOR showed a lower staining for Bax, whereas positive staining was observed for Bcl-2. Scale bar: 100 μm; objective 10×. $^{***}p < 0.001$, $^{****}p < .0001$ [Colour figure can be viewed at wileyonlinelibrary.com]

did not show positive staining for Bax, cleaved caspase 3, and caspase 9 (Figures 4 and 5).

On the contrary, Bcl-2, a well-known anti-apoptotic protein, was not expressed in SCI spinal cord tissues, but positive staining was detected in both SCI mice injected with GMSCs and GMSCs + MOR (Figure 4). In particular, in the spinal cord of SCI mice injected with GMSCs + MOR, the Bcl-2 level was similar to that of sham animals (Figure 4).

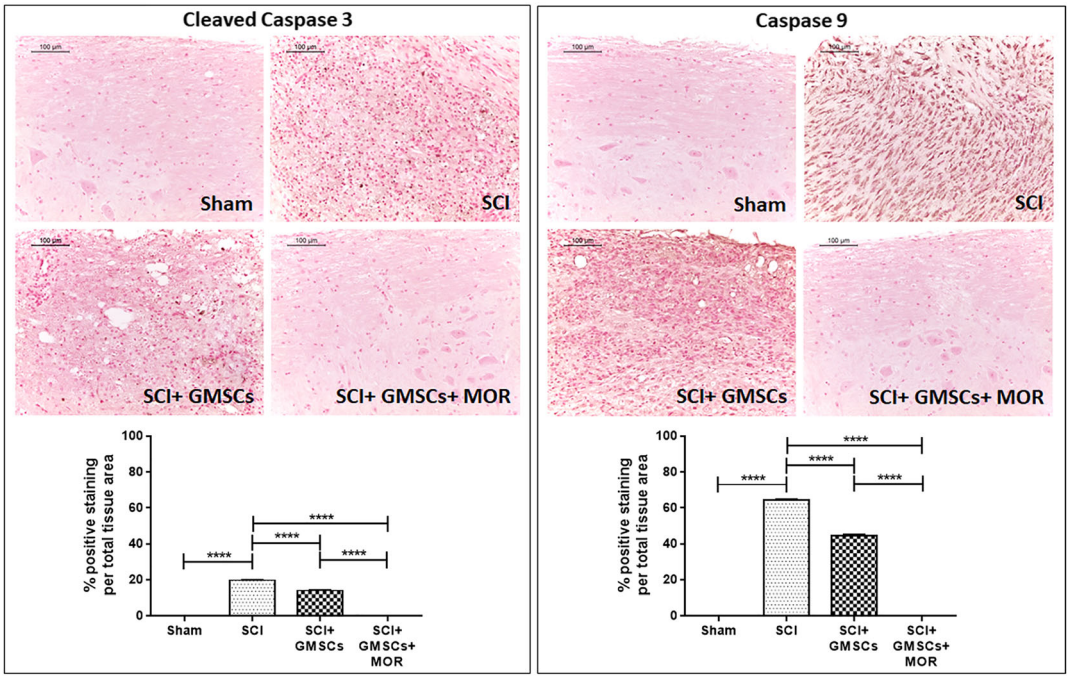


**FIGURE 5** Immunohistochemistry for cleaved caspase 3 and caspase 9 with densitometric analysis. Immunohistochemistry evidenced the positive staining for both markers in the spinal cord of SCI mice compared with sham animals, where negative staining was observed. SCI mice administered with GMSCs showed a lower staining compared with SCI mice, whereas GMSCs + MOR showed negative staining for cleaved caspase 3 and caspase 9. Scale bar: 100 μm; objective 10×. $^{****}p < .0001$ [Colour figure can be viewed at wileyonlinelibrary.com]

These results indicated that GMSCs are able to reduce apoptosis, but pretreatment with MOR was able to potentiate their action, resulting in the inhibition of apoptosis.

### 3.5 | GMSCs pretreated with MOR expressed anti-inflammatory cytokines

In order to characterize the mechanism of action of GMSCs treated with MOR, we investigated in vitro the effects of MOR on GMSCs. At first, we observed that GMSCs treated with MOR for 48 hr showed more marked staining for IL-10 and TGF-β compared with GMSCs in basal condition (Figure 6). On the contrary, GMSCs treated with MOR did not express for COX-2, IL-1β and MMP9, and p38 (Figure 6). Western blot of precipitated protein from the cell culture medium showed significantly increased expression levels of TGF-β and IL-10 in the medium of GMSCs treated with MOR compared with the medium of cells in basal condition (Figure 6).

## 4 | DISCUSSION

The use of GMSCs may be a promising therapeutic strategy in SCI. SCI is a neurological disorder that affects 1.3 million persons worldwide. The neurological damages have a significant negative impact on the quality of life in the affected patients. Despite intense research, SCI still represents an unmet medical need, mostly due to the low regenerative capacity of spinal neurons. Steroids have been considered as one of the potential interventions in the management of SCI for their anti-inflammatory function. However, steroid treatment has been shown to improve some aspects of neurologic outcome in humans if administered within 8 hr of injury (Bracken, 2012).

Several preclinical experiments report the efficacy of stem cell therapy to improve motor activity when administrated into murine SCI models obtained via compression, contusion, or transaction of the spinal cord (Dasari, Veeravalli, & Dinh, 2014). Moreover, MSCs can provide immunomodulation and trophic support in SCI, as they can release many potential beneficial factors at the damaged tissue site (Vismara, Papa, Rossi, Forloni, & Veglianese, 2017).

Several independent studies have shown the immunomodulatory and anti-inflammatory effects of MSCs; they are able to regulate the immune system by inhibiting the proliferation of T and B cells (Augello et al., 2005), natural killer cells signaling (Aggarwal & Pittenger, 2005), reduce apoptosis, and influencing the production of pro-inflammatory and anti-inflammatory cytokines (Salami, Tavassoli, Mehrzad, & Parham, 2018). The inflammatory responses play a central role in the pathogenesis of SCI and lesions, contributing in regenerative processes, and can also induce apoptosis of neurons and oligodendrocytes and the loss of neuronal function (Genovese et al., 2009; Zhang, Yin, Xu, Wu, & Chen, 2012). Furthermore, GMSCs have been shown to be a promising source able to replace neurons lost because of their natural ability to differentiate into neural precursor cells over prolonged passages (Rajan, Scionti, et al., 2017).

In our previous studies, we already demonstrated the anti-inflammatory effect of phyto-compounds of *M. oleifera* in neuroinflammatory and neurodegenerative diseases (Giacoppo et al., 2016; Giacoppo, Rajan, et al., 2017). We have also shown the ability

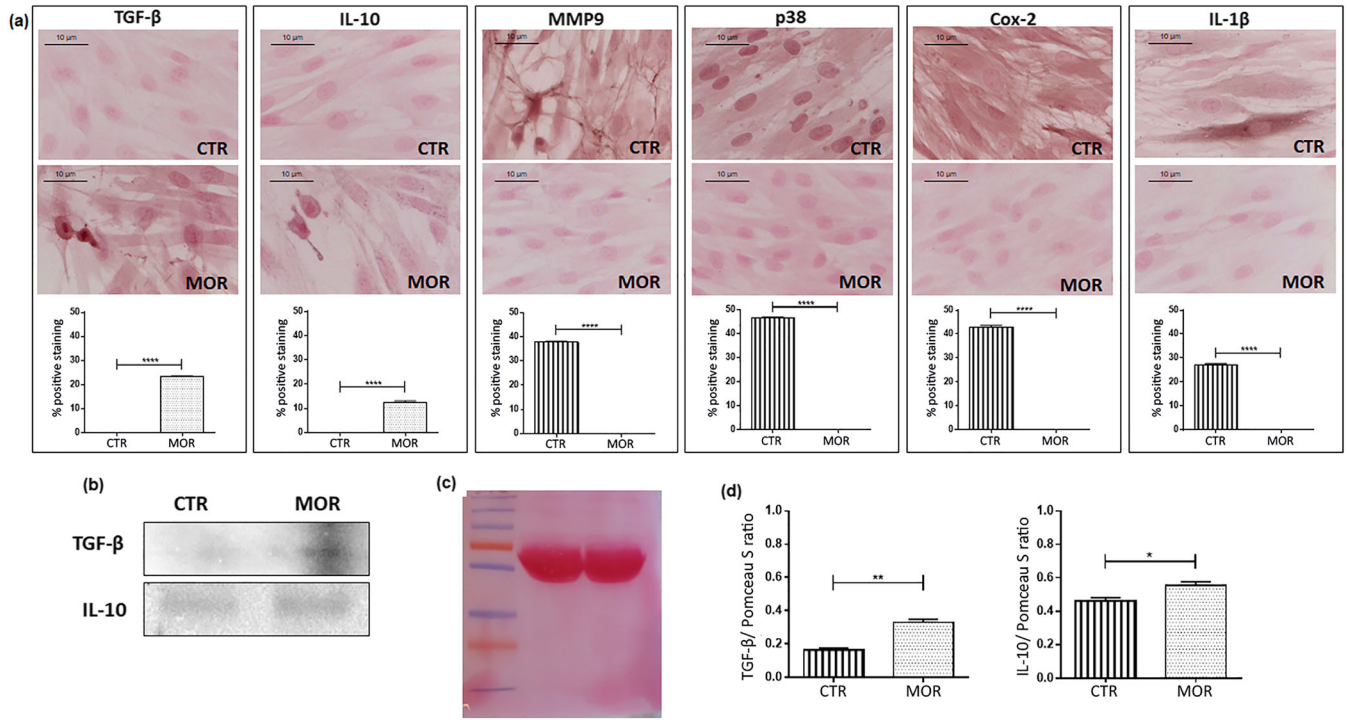


**FIGURE 6** Immunocytochemistry for TGF-β, IL-10, MMP9, p38, COX-2, and IL-1β in GMSCs and western blot analysis for TGF-β and IL-10 on the protein precipitated from the cell culture medium. (a) Immunocytochemistry evidenced the positive staining for the anti-inflammatory cytokines TGF-β and IL-10 in GMSCs treated with MOR compared with untreated cells, where negative staining was observed. Immunocytochemistry evidenced the positive staining for MMP9, p38, COX-2, and IL-1β in GMSCs cultured in basal condition, whereas GMSCs treated with MOR showed negative staining. Magnification: 100×. Scale bar: 10 μm. $^{****}p < .0001$. (b) Western blot analysis showed increased levels of TGF-β and IL-10 in the cell culture medium of GMSCs treated with MOR. (c) Ponceau S staining was used as a loading control. (d) Densitometric analysis. $^{*}p < .05$, $^{**}p < .01$ [Colour figure can be viewed at wileyonlinelibrary.com]

of MOR treatment to accelerate the neuronal differentiation process in periodontal ligament stem cells as demonstrated by the up-regulation of neural-related markers, such as GAP43, p75, BDNF, and NESTIN (Romeo et al., 2018). However, MOR, as well as other isothiocyanates, is not soluble in water that results in stability problems for the delivery. This difficulty, as we previously described, can be overcome by complexation of MOR with cyclodextrins, cyclic oligosaccharides able to form water–soluble inclusion complexes with small molecules (Giacoppo, Iori, Rollin, Bramanti, & Mazzon, 2017; Mathiron et al., 2018). In this work, we proposed the liposomes as another moringin formulation able to improve its solubility and stability in an aqueous medium. Liposomes, in fact, for their unique bilayer structure, are well recognized as drug-delivery vehicles and are widely used as carriers for both lipophilic and hydrophilic molecules (Bozzuto & Molinari, 2015). Our results evidenced the embedding of MOR in the liposomes. Furthermore, MOR, solubilized in the liposome bilayer, did not alter liposomes features significantly and only slightly increased their dimension. Through the evaluation of CF internalization, we observed that liposomes were localized in the cytoplasm, in particular, in the perinuclear area, but a slight fluorescence was visible also in the nucleus. We evidenced an increased ability of GMSCs pretreated with MOR-enriched liposomes to induce remodeling of cytoskeleton arrangement, as demonstrated to SEM morphological evaluation. In fact, several cells acquire a roundish morphology with the transformation of elongation process in short filopodia.

The principal aim of SCI therapy is to re-establish the normal spinal cord morphology, to improve motor function and to modulate the inflammatory and apoptotic processes associated with SCI. In particular, GMSCs treatment has significantly improved the motor function in SCI mice from Day 8 post-trauma, whereas GMSCs–MOR treatment showed faster recovery yet from Day 4 post-injury. SCI mice exhibited higher levels of pro-inflammatory cytokines IL-1β and IL-6 and COX-2. The administration of GMSCs alone reduced the levels of these pro-inflammatory markers. However, MOR pretreatment enhances the effect of GMSCs inducing a further reduction of the expression of these ILs (IL-6 and IL-1β) in SCI mice. It has been reported that pro-inflammatory cytokines, including IL-1β and IL-6, are induced rapidly following SCI. IL-1β is mainly secreted by activated microglia/macrophages in response to injury, and the expression of other cytokines, such as IL-6, and COX-2 protein is induced that are implicated in the inflammatory response to injury (Garcia, Aguilar-Cevallos, Silva-Garcia, & Ibarra, 2016; Glass, Saijo, Winner, Marchetto, & Gage, 2010).

In our study, we also observed higher levels of GFAP in the spinal cord of SCI mice compared with sham. Increased expression of GFAP is considered a marker of reactive astrocyte (Pekny & Pekna, 2004),

and GFAP elevation has already been reported after SCI (Goldshmit et al., 2015). However, the treatment with GMSCs pretreated with MOR reduced its levels.

The link between inflammation and apoptosis is already known (Zhang et al., 2012). Indeed, in our study, we found in SCI animals the induction of apoptosis associated with the presence of the inflammatory cytokines, IL-1β, IL-6, and COX-2 proteins. GMSCs were able to reduce apoptosis, but pretreatment with MOR was able to potentiate their action. In our work, the anti-apoptotic effect exerted by GMSCs pretreated with MOR results in a reduction of Bax and inhibition of pro-apoptotic proteins caspase 9 and cleaved caspase 3 and, in parallel, in an increased expression of the anti-apoptotic Bcl-2 protein.

These results may be explained taking into account that GMSCs in vitro release the immunoregulatory cytokines TGF-β and IL-10, as demonstrated in our previous work (Rajan, Diomede, Bramanti, Trubiani, & Mazzon, 2017), but interestingly, the treatment with MOR increases their expression levels as demonstrated both in precipitated culture medium and in situ by immunocytochemistry. Moreover, the immunocytochemistry shows that MOR treatment reduces the IL-1β expression and consequently the MMP9 and p38 levels blocking MAPK pathway (Liang et al., 2007), another mechanism whereby the MOR can also reduce oxidative damage and inflammation involved in SCI.

The results imply that GMSCs, in an inflammatory environment, suppress pro-inflammatory responses, modulate the immune system, inhibit apoptosis, and stimulate tissue-intrinsic progenitor cell differentiation. The observation that GMSCs–MOR treatment reduced the morphological abnormalities of the spinal cord, improved the recovery of motor function, and inhibited the activation of the apoptotic process further support their potential exploitation in SCI. Stem cells enriched with nanostructured liposomes containing moringin could represent a new interesting approach to enhance the performance of stem cells therapy in the management of SCI.

## ACKNOWLEDGEMENTS

This study was supported by current research funds 2018 of IRCCS "Centro Neurolesi Bonino-Pulejo," Messina, Italy. Authors thank Dr. Alessia Ventrella (University "G. D'Annunzio"), for her support in liposomes development and analyses.

## AUTHOR CONTRIBUTIONS

Santa Mammana and Eugenio Cavalli performed in vivo experiments. Santa Mammana and Agnese Gugliandolo wrote the manuscript and performed and analyzed western blot. Francesca Diomede isolated GMSCs and performed and analyzed in vitro experiments. Renato Iori provided moringin. Romina Zappacosta and Antonella Fontana characterized liposomes. Jacopo Pizzicannella and Emanuela Mazzon designed the research. Emanuela Mazzon performed immunohistochemistry and immunocytochemistry. Placido Bramanti provided funding. Pio Conti critically revised the manuscript.

## CONFLICT OF INTEREST

The authors have declared that there is no conflict of interest.

## ORCID

*Emanuela Mazzon* https://orcid.org/0000-0002-5073-717X

## REFERENCES

Aggarwal, S., & Pittenger, M. F. (2005). Human mesenchymal stem cells modulate allogeneic immune cell responses. *Blood*, *105*(4), 1815–1822. https://doi.org/10.1182/blood-2004-04-1559

Ahuja, C. S., Nori, S., Tetreault, L., Wilson, J., Kwon, B., Harrop, J., … Fehlings, M. G. (2017). Traumatic spinal cord injury-repair and regeneration. *Neurosurgery*, *80*(3S), S9–S22. https://doi.org/10.1093/neuros/nyw080

Augello, A., Tasso, R., Negrini, S. M., Amateis, A., Indiveri, F., Cancedda, R., & Pennesi, G. (2005). Bone marrow mesenchymal progenitor cells inhibit lymphocyte proliferation by activation of the programmed death 1 pathway. *European Journal of Immunology*, *35*(5), 1482–1490. https://doi.org/10.1002/eji.200425405

Ballerini, P., Diomede, F., Petragnani, N., Cicchitti, S., Merciaro, I., Cavalcanti, M., & Trubiani, O. (2017). Conditioned medium from relapsing-remitting multiple sclerosis patients reduces the expression and release of inflammatory cytokines induced by LPS-gingivalis in THP-1 and MO3.13 cell lines. *Cytokine*, *96*, 261–272. https://doi.org/10.1016/j.cyto.2017.04.022

Basso, D. M., Fisher, L. C., Anderson, A. J., Jakeman, L. B., McTigue, D. M., & Popovich, P. G. (2006). Basso mouse scale for locomotion detects differences in recovery after spinal cord injury in five common mouse strains. *Journal of Neurotrauma*, *23*(5), 635–659. https://doi.org/10.1089/neu.2006.23.635

Bozzuto, G., & Molinari, A. (2015). Liposomes as nanomedical devices. *International Journal of Nanomedicine*, *10*, 975–999. https://doi.org/10.2147/Ijn.S68861

Bracken, M. B. (2012). Steroids for acute spinal cord injury. *Cochrane Database of Systematic Reviews*, (1), CD001046. https://doi.org/10.1002/14651858.CD001046.pub2

Bracken, M. B., Shepard, M. J., Holford, T. R., Leo-Summers, L., Aldrich, E. F., Fazl, M., … Young, W. (1997). Administration of methylprednisolone for 24 or 48 hours or tirilazad mesylate for 48 hours in the treatment of acute spinal cord injury. Results of the Third National Acute Spinal Cord Injury Randomized Controlled Trial. National Acute Spinal Cord Injury Study. *Jama*, *277*(20), 1597–1604.

Brunelli, D., Tavecchio, M., Falcioni, C., Frapolli, R., Erba, E., Iori, R., … D'Incalci, M. (2010). The isothiocyanate produced from glucomoringin inhibits NF-κB and reduces myeloma growth in nude mice in vivo. *Biochemical Pharmacology*, *79*(8), 1141–1148. https://doi.org/10.1016/j.bcp.2009.12.008

Cavalcanti, M. F., Maria, D. A., de Isla, N., Leal-Junior, E. C., Joensen, J., Bjordal, J. M., … Frigo, L. (2015). Evaluation of the proliferative effects induced by low-level laser therapy in bone marrow stem cell culture. *Photomedicine and Laser Surgery*, *33*(12), 610–616. https://doi.org/10.1089/pho.2014.3864

Dasari, V. R., Veeravalli, K. K., & Dinh, D. H. (2014). Mesenchymal stem cells in the treatment of spinal cord injuries: A review. *World Journal of Stem Cells*, *6*(2), 120–133. https://doi.org/10.4252/wjsc.v6.i2.120

De Maria, P., Fontana, A., Gasbarri, C., & Velluto, D. (2006). Effects of fullerene guests on the stability of 1-palmitoyl-2-oleoylphosphatidylcholine liposomes. *Soft Matter*, *2*, 595. https://doi.org/10.1039/b603266d

Diomede, F., Gugliandolo, A., Scionti, D., Merciaro, I., Cavalcanti, M. F., Mazzon, E., & Trubiani, O. (2018). Biotherapeutic effect of gingival stem cells conditioned medium in bone tissue restoration. *International Journal of Molecular Sciences*, *19*(2). https://doi.org/10.3390/ijms19020329

Diomede, F., Merciaro, I., Martinotti, S., Cavalcanti, M. F., Caputi, S., Mazzon, E., & Trubiani, O. (2016). miR-2861 is involved in osteogenic commitment of human periodontal ligament stem cells grown onto 3D scaffold. *Journal of Biological Regulators and Homeostatic Agents*, *30*(4), 1009–1018.

Diomede, F., Rajan, T. S., Gatta, V., D'Aurora, M., Merciaro, I., Marchisio, M., … Trubiani, O. (2017). Stemness maintenance properties in human oral stem cells after long-term passage. *Stem Cells International*, *2017*, 1, 14. 5651287. https://doi.org/10.1155/2017/5651287

Diomede, F., Zingariello, M., Cavalcanti, M., Merciaro, I., Pizzicannella, J., De Isla, N., … Trubiani, O. (2017). MyD88/ERK/NFκB pathways and pro-inflammatory cytokines release in periodontal ligament stem cells stimulated by *Porphyromonas gingivalis*. *European Journal of Histochemistry*, *61*(2), 2791. https://doi.org/10.4081/ejh.2017.2791

Diomede, F., Zini, N., Pizzicannella, J., Merciaro, I., Pizzicannella, G., D'Orazio, M., … Trubiani, O. (2018). 5-Aza exposure improves reprogramming process through embryoid body formation in human gingival stem cells. *Front Genet*, *9*, 419. https://doi.org/10.3389/fgene.2018.00419

Egusa, H., Sonoyama, W., Nishimura, M., Atsuta, I., & Akiyama, K. (2012). Stem cells in dentistry—Part II: Clinical applications. *Journal of Prosthodontic Research*, *56*(4), 229–248. https://doi.org/10.1016/j.jpor.2012.10.001

Garcia, E., Aguilar-Cevallos, J., Silva-Garcia, R., & Ibarra, A. (2016). Cytokine and growth factor activation in vivo and in vitro after spinal cord injury. *Mediators of Inflammation*, *2016*, 1, 21. 9476020. https://doi.org/10.1155/2016/9476020

Genovese, T., Esposito, E., Mazzon, E., Di Paola, R., Caminiti, R., Bramanti, P., … Cuzzocrea, S. (2009). Absence of endogenous interleukin-10 enhances secondary inflammatory process after spinal cord compression injury in mice. *Journal of Neurochemistry*, *108*(6), 1360–1372. https://doi.org/10.1111/j.1471-4159.2009.05899.x

Giacoppo, S., Iori, R., Rollin, P., Bramanti, P., & Mazzon, E. (2017). Moringa isothiocyanate complexed with α-cyclodextrin: A new perspective in neuroblastoma treatment. *BMC Complementary and Alternative Medicine*, *17*(1), 362. https://doi.org/10.1186/s12906-017-1876-z

Giacoppo, S., Rajan, T. S., De Nicola, G. R., Iori, R., Rollin, P., Bramanti, P., & Mazzon, E. (2017). The isothiocyanate isolated from *Moringa oleifera* shows potent anti-inflammatory activity in the treatment of murine subacute Parkinson's disease. *Rejuvenation Research*, *20*(1), 50–63. https://doi.org/10.1089/rej.2016.1828

Giacoppo, S., Soundara Rajan, T., De Nicola, G. R., Iori, R., Bramanti, P., & Mazzon, E. (2016). Moringin activates Wnt canonical pathway by inhibiting GSK3β in a mouse model of experimental autoimmune encephalomyelitis. *Drug Design, Development and Therapy*, *10*, 3291–3304. https://doi.org/10.2147/DDDT.S110514

Giacoppo, S., Thangavelu, S. R., Diomede, F., Bramanti, P., Conti, P., Trubiani, O., & Mazzon, E. (2017). Anti-inflammatory effects of hypoxia-preconditioned human periodontal ligament cell secretome in an experimental model of multiple sclerosis: A key role of IL-37. *The FASEB Journal*, *31*(12), 5592–5608. https://doi.org/10.1096/fj.201700524R

Glass, C. K., Saijo, K., Winner, B., Marchetto, M. C., & Gage, F. H. (2010). Mechanisms underlying inflammation in neurodegeneration. *Cell*, *140*(6), 918–934. https://doi.org/10.1016/j.cell.2010.02.016

Goldshmit, Y., Kanner, S., Zacs, M., Frisca, F., Pinto, A. R., Currie, P. D., & Pinkas-Kramarski, R. (2015). Rapamycin increases neuronal survival, reduces inflammation and astrocyte proliferation after spinal cord injury. *Molecular and Cellular Neuroscience*, *68*, 82–91. https://doi.org/10.1016/j.mcn.2015.04.006

Hendijani, F. (2017). Explant culture: An advantageous method for isolation of mesenchymal stem cells from human tissues. *Cell Proliferation*, *50*(2). https://doi.org/10.1111/cpr.12334

Liang, K. C., Lee, C. W., Lin, W. N., Lin, C. C., Wu, C. B., Luo, S. F., & Yang, C. M. (2007). Interleukin-1β induces MMP-9 expression via p42/44 MAPK, p38 MAPK, JNK, and nuclear factor-κB signaling pathways in human tracheal smooth muscle cells. *Journal of Cellular Physiology*, *211*(3), 759–770. https://doi.org/10.1002/jcp.20992

Libro, R., Scionti, D., Diomede, F., Marchisio, M., Grassi, G., Pollastro, F., … Trubiani, O. (2016). Cannabidiol modulates the immunophenotype and inhibits the activation of the inflammasome in human gingival mesenchymal stem cells. *Frontiers in Physiology*, *7*, 559. https://doi.org/10.3389/fphys.2016.00559

Mahla, R. S. (2016). Stem cells applications in regenerative medicine and disease therapeutics. *International Journal of Cell Biology*, *2016*, 1, 24. 6940283. https://doi.org/10.1155/2016/6940283

Manconi, M., Isola, R., Falchi, A. M., Sinico, C., & Fadda, A. M. (2007). Intracellular distribution of fluorescent probes delivered by vesicles of different lipidic composition. *Colloids and Surfaces. B, Biointerfaces*, *57*(2), 143–151. https://doi.org/10.1016/j.colsurfb.2007.01.016

Mathiron, D., Iori, R., Pilard, S., Soundara Rajan, T., Landy, D., Mazzon, E., … Djedaini-Pilard, F. (2018). A combined approach of nmr and mass spectrometry techniques applied to the α-cyclodextrin/moringin complex for a novel bioactive formulation (dagger). *Molecules*, *23*(7). https://doi.org/10.3390/molecules23071714

Muller, C., van Loon, J., Ruschioni, S., De Nicola, G. R., Olsen, C. E., Iori, R., & Agerbirk, N. (2015). Taste detection of the non-volatile isothiocyanate moringin results in deterrence to glucosinolate-adapted insect larvae. *Phytochemistry*, *118*, 139–148. https://doi.org/10.1016/j.phytochem.2015.08.007

Nakamura, M., Houghtling, R. A., MacArthur, L., Bayer, B. M., & Bregman, B. S. (2003). Differences in cytokine gene expression profile between acute and secondary injury in adult rat spinal cord. *Experimental Neurology*, *184*(1), 313–325. https://doi.org/10.1016/S0014-4886(03)00361-3

Oliveri, R. S., Bello, S., & Biering-Sorensen, F. (2014). Mesenchymal stem cells improve locomotor recovery in traumatic spinal cord injury: Systematic review with meta-analyses of rat models. *Neurobiology of Disease*, *62*, 338–353. https://doi.org/10.1016/j.nbd.2013.10.014

Pekny, M., & Pekna, M. (2004). Astrocyte intermediate filaments in CNS pathologies and regeneration. *Journal of Pathology*, *204*(4), 428–437. https://doi.org/10.1002/path.1645

Phinney, D. G., & Prockop, D. J. (2007). Concise review: Mesenchymal stem/multipotent stromal cells: The state of transdifferentiation and modes of tissue repair—Current views. *Stem Cells*, *25*(11), 2896–2902. https://doi.org/10.1634/stemcells.2007-0637

Pizzicannella, J., Cavalcanti, M., Trubiani, O., & Diomede, F. (2018). MicroRNA 210 mediates VEGF upregulation in human periodontal ligament stem cells cultured on 3D hydroxyapatite ceramic scaffold. *International Journal of Molecular Sciences*, *19*(12). https://doi.org/10.3390/ijms19123916

Pizzicannella, J., Diomede, F., Merciaro, I., Caputi, S., Tartaro, A., Guarnieri, S., & Trubiani, O. (2018). Endothelial committed oral stem cells as modelling in the relationship between periodontal and cardiovascular disease. *Journal of Cellular Physiology*, *233*(10), 6734–6747. https://doi.org/10.1002/jcp.26515

Pizzicannella, J., Rabozzi, R., Trubiani, O., & Di Giammarco, G. (2011). Histidine-tryptophan-ketoglutarate solution helps to preserve endothelial integrity of saphenous vein: An immunohistochemical and ultrastructural analysis. *Journal of Biological Regulators and Homeostatic Agents*, *25*(1), 93–99.

Rajan, T. S., Diomede, F., Bramanti, P., Trubiani, O., & Mazzon, E. (2017). Conditioned medium from human gingival mesenchymal stem cells protects motor-neuron-like NSC-34 cells against scratch-injury-induced cell death. *International Journal of Immunopathology and Pharmacology*, *30*(4), 383–394. https://doi.org/10.1177/0394632017740976

Rajan, T. S., Scionti, D., Diomede, F., Piattelli, A., Bramanti, P., Mazzon, E., & Trubiani, O. (2017). Prolonged expansion induces spontaneous neural progenitor differentiation from human gingiva-derived mesenchymal stem cells. *Cellular Reprogramming*, *19*(6), 389–401. https://doi.org/10.1089/cell.2017.0012

Romeo, L., Diomede, F., Gugliandolo, A., Scionti, D., Lo Giudice, F., Lanza Caricchio, V., … Mazzon, E. (2018). Moringin induces neural differentiation in the stem cell of the human periodontal ligament. *Scientific Reports*, *8*(1), 9153. https://doi.org/10.1038/s41598-018-27492-0

Salami, F., Tavassoli, A., Mehrzad, J., & Parham, A. (2018). Immunomodulatory effects of mesenchymal stem cells on leukocytes with emphasis on neutrophils. *Immunobiology*, *223*(12), 786–791. https://doi.org/10.1016/j.imbio.2018.08.002

Sharpe, P. T. (2016). Dental mesenchymal stem cells. *Development*, *143*(13), 2273–2280. https://doi.org/10.1242/dev.134189

Shende, P., & Subedi, M. (2017). Pathophysiology, mechanisms and applications of mesenchymal stem cells for the treatment of spinal cord injury. *Biomedicine & Pharmacotherapy*, *91*, 693–706. https://doi.org/10.1016/j.biopha.2017.04.126

Singh, P. L., Agarwal, N., Barrese, J. C., & Heary, R. F. (2012). Current therapeutic strategies for inflammation following traumatic spinal cord injury. *Neural Regeneration Research*, *7*(23), 1812–1821. https://doi.org/10.3969/j.issn.1673-5374.2012.23.008

Velluto, D., Gasbarri, C., Angelini, G., & Fontana, A. (2011). Use of simple kinetic and reaction-order measurements for the evaluation of the mechanism of surfactant-liposome interactions. *The Journal of Physical Chemistry. B*, *115*(25), 8130–8137. https://doi.org/10.1021/jp2026187

Via, A. G., Frizziero, A., & Oliva, F. (2012). Biological properties of mesenchymal stem cells from different sources. *Muscle, Ligaments and Tendons Journal*, *2*(3), 154–162.

Viale, M., Fontana, A., Maric, I., Monticone, M., Angelini, G., & Gasbarri, C. (2016). Preparation and antiproliferative activity of liposomes containing a combination of cisplatin and procainamide hydrochloride. *Chemical Research in Toxicology*, *29*(9), 1393–1395. https://doi.org/10.1021/acs.chemrestox.6b00207

Vismara, I., Papa, S., Rossi, F., Forloni, G., & Veglianese, P. (2017). Current options for cell therapy in spinal cord injury. *Trends in Molecular Medicine*, *23*(9), 831–849. https://doi.org/10.1016/j.molmed.2017.07.005

Volkman, R., & Offen, D. (2017). Concise review: Mesenchymal stem cells in neurodegenerative diseases. *Stem Cells*, *35*(8), 1867–1880. https://doi.org/10.1002/stem.2651

Wang, S., Qu, X., & Zhao, R. C. (2011). Mesenchymal stem cells hold promise for regenerative medicine. *Frontiers in Medicine*, *5*(4), 372–378. https://doi.org/10.1007/s11684-011-0164-4

Xu, X., Chen, C., Akiyama, K., Chai, Y., Le, A. D., Wang, Z., & Shi, S. (2013). Gingivae contain neural-crest- and mesoderm-derived mesenchymal stem cells. *Journal of Dental Research*, *92*(9), 825–832. https://doi.org/10.1177/0022034513497961

Zappacosta, R., Semeraro, M., Baroncini, M., Silvi, S., Aschi, M., Credi, A., & Fontana, A. (2010). Liposome destabilization by a 2,7-diazapyrenium derivative through formation of transient pores in the lipid bilayer. *Small*, *6*(8), 952–959. https://doi.org/10.1002/smll.200902306

Zhang, N., Yin, Y., Xu, S. J., Wu, Y. P., & Chen, W. S. (2012). Inflammation & apoptosis in spinal cord injury. *The Indian Journal of Medical Research*, *135*, 287–296.

Zhao, Q., Ren, H., & Han, Z. (2016). Mesenchymal stem cells: Immunomodulatory capability and clinical potential in immune diseases. *Journal of Cellular Immunotherapy*, *2*, 3–20. https://doi.org/10.1016/j.jocit.2014.12.001

**How to cite this article:** Mammana S, Gugliandolo A, Cavalli E, et al. Human gingival mesenchymal stem cells pretreated with vesicular moringin nanostructures as a new therapeutic approach in a mouse model of spinal cord injury. *J Tissue Eng Regen Med*. 2019;13:1109–1121. https://doi.org/10.1002/term.2857